

Analysis of stellar spectra with 3D and NLTE models

Maria Bergemann

Abstract Models of radiation transport in stellar atmospheres are the hinge of modern astrophysics. Our knowledge of stars, stellar populations, and galaxies is only as good as the theoretical models, which are used for the interpretation of their observed spectra, photometric magnitudes, and spectral energy distributions. I describe recent advances in the field of stellar atmosphere modelling for late-type stars. Various aspects of radiation transport with 1D hydrostatic, LTE, NLTE, and 3D radiative-hydrodynamical models are briefly reviewed.

1 Introduction

Models of stellar atmospheres and spectral line formation are a crucial part of observational astrophysics. The models are our ultimate link between observations of stars and their fundamental physical parameters. On the one side, the models allow us to go from observable quantities, i.e. stellar fluxes, spectral energy distributions, and photometric magnitudes, to physical parameters of stars, such as effective temperature T_{eff} , surface gravity $\log g$, metallicity $[\text{Fe}/\text{H}]$, abundances, rotation and turbulent velocities. The atmospheric models also allow us to convert theoretical bolometric luminosities from stellar evolution models to their observable quantities, theoretical colours, which are then compared with observations. E.g., model vs observed colour-magnitude diagrams are used to determine distances and ages of clusters and field stars. The shapes of stellar energy distributions (SED) serve as a diagnostics of inter-stellar and circumstellar reddening. There are mass- and age-sensitive diagnostics in stellar spectrum, such as the ultra-violet Ca H and K lines, which may help to tell a young star from an old star. Detailed chemical abundances are arguably the most important physical quantities, which can be only deciphered

M. Bergemann
Institute of Astronomy, University of Cambridge, Madingley Road, CB3 0HA, Cambridge, UK
e-mail: mbergema@ast.cam.ac.uk

from a stellar spectrum. They link stellar properties to nucleosynthesis of elements in the Big Bang, in stars at the end of their life-times, in violent explosions, caused by stellar interactions, and by cosmic ray acceleration in the interstellar medium. This connection forms the basis of important diagnostics methods to constrain formation and evolution of stars, stellar populations, and galaxies.

In short, all fundamental physical stellar quantities critically depend on the models we use for the analysis of observations. Until recently, we could only use the simplest 1D hydrostatic models in local thermodynamic equilibrium (LTE) for stellar parameter determinations, for more sophisticated models were far too computationally expensive. Calculation of a 3D radiative-hydrodynamical (3D RHD) model required months of CPU time, which was of little use for any practical application in spectroscopic analysis. Moreover, the accurate solution of radiation transport even in the time-independent scheme has been too demanding for quantitative applications. Non-local thermodynamic equilibrium (NLTE) calculations were disfavoured for several reasons. First, inversion of large matrices in the complete linearisation scheme (for solving coupled statistical equilibrium equations in non-LTE) was prohibitive for atoms with complex atomic structure. Furthermore, lack of accurate ab initio calculations or experimental atomic data lead to the need to introduce simplified treatment of several types of atomic processes in vastly more complex non-LTE calculations, which caused a wide-spread misconception that non-LTE calculations are of questionable advantage.

It is crucial to realise that non-LTE is not an approximation, in contrast to LTE, which approximates all collision rates by the infinitely large numbers, and fully ignores the influence of radiation field in stellar atmospheres on the energy distribution of matter. One may however, solve time-dependent rate equations, or drop the time dependence, which reduces the problem to solving the equations of statistical equilibrium only (see below).

However, the theory of radiative transfer in stellar atmospheres is one of the most mature fields in astrophysics (e.g. the fundamental work by Mihalas 1979) and the numerical implementation of the theory has seen substantial improvement over the past decade. Moreover, we have enough computational power to simulate stellar convection in 3D and solve for radiative transfer explicitly taking into account the interaction of gas particles with the radiation field. In this lecture I summarise the main progress in modelling atmospheres and spectra of cool, FGKM, stars, that has been made during the past decade, and provide a timeline for the developments in the field which can be expected in the near future. I do not touch upon the problems of radiative transfer in more complex cases, such as expanding supernova shells (Lucy, 1999) or dusty AGB envelopes (Höfner et al, 2003, and ref. therein), or chromospheres (e.g. Hansteen et al, 2007).

2 Basic considerations

The analysis of cool FGK stars meets with two main kinds of difficulties. These stars have sub-surface convection zone and radiation field in their photospheres is highly non-local. As a consequence, neither of the two classical modelling approximations, LTE and 1D hydrostatic equilibrium, is valid and cannot be justified without detailed *ab initio* theoretical calculations. An excellent review of NLTE and 3D simulations from a theoretical perspective is given in the Annual Review articles by Mihalas and Athay (1973) and Spruit et al (1990); a comprehensive summary of 3D and NLTE in application to stellar abundance analysis is provided in Asplund (2005).

What is the reason for NLTE? A star is not a perfect black-body and radiation field influences the physical state of matter and vice versa. Therefore, only consistent NLTE radiative transfer will correctly recover the thermodynamic structure of the atmosphere and thus the properties of its radiation field. In NLTE, the particle distribution functions, i.e. the excitation and ionisation states, are influenced by the radiation field that causes them to depart from the LTE values. Why this happens is easy to understand. Stellar atmosphere is the region where radiation escapes into ISM. Deep in the atmospheres, opacity is large and the photon mean free path is very small. Radiation transport occurs over very small length scales, thus connecting gas parcels with very similar thermodynamic properties.

The definition of a *stellar surface* is somewhat vague. Strictly speaking, this is the boundary where material at the most transparent wavelength λ becomes optically thin, $\tau_\lambda < 1$. This wavelength is $1.6\mu\text{m}$, where the H^- opacity in continuum is at its minimum, however, in practice this wavelength is rarely used. It is more common to refer to the $\lambda = 500\text{ nm}$, where most of the flux is emitted by a typical solar-like star, or to the Rosseland mean opacity, a Planck-function weighted average over all frequencies.

Photon mean free path is the length scale over which thermalisation takes place.

However, closer to the stellar surface photon mean free path λ_p becomes large, larger than the scale height of material. Thus, as we move outwards, the decoupling between radiation and matter increases, radiation becomes non-local, anisotropic, and strongly non-Planckian. Many spectral lines form in NLTE showing shapes which bear no resemblance with the line profiles predicted by classical LTE models. For example, the Mg I line at $12\mu\text{m}$ reverts to emission at the solar limb that can be only accounted for by NLTE models. The effect on other spectral features is less obvious, although it may still dramatically impact the line equivalent widths and their detailed profiles, i.e. the total energy absorbed in a line (see next Section).

Another major source of complexity is convection. There are several observable manifestations of stellar convection, the most prominent is stellar surface granulation, which has been in the focus of observational research for more than a decade. Fig. 1 shows a patch on the solar surface observed with the Swedish Solar Telescope

telescope. The intensity fluctuations correspond to brighter granules and darker inter-granular lanes. The brightness fluctuations are about 20%, while the actual temperature contrast across the granulation pattern is about 25%. This mild dependence of surface intensity variation on T is caused by the huge sensitivity of H^- continuum opacity to the temperature. The other key observable are the characteristic C- and inverse C- shaped bisectors of the line profiles that are caused by up- and down-flows (e.g. Gray et al, 2008). The bisectors can be best observed in the very high-quality solar spectrum (Fig. 2).

Indeed, these beautiful observations motivated the development of complex 3D radiative hydrodynamics (RHD) models (Nordlund et al, 2009) and even larger solar telescopes, such as, e.g., the new German 1.5m GREGOR telescope. Inhomogeneities, spots, and convective motions were also resolved on the surfaces of red supergiants (Buscher et al, 1990; Wilson et al, 1992; Tuthill et al, 1997; Wilson et al, 1997; Young et al, 2000; Haubois et al, 2009; Ohnaka et al, 2009; Kervella et al, 2009; Ohnaka et al, 2011, also see the first lecture in this series). More interesting results about atmospheric structure and dynamics of cool stars will soon come to light with new telescopes and missions, such as the Herschel Space Observatory (Teyssier et al, 2012). All these data will need complex theoretical models to understand the physics underlying the observed phenomena.

3 Theory

What we are trying to understand is how the stellar light we detect with our instruments, e.g. in the form of a spectrum, is created in a stellar atmosphere. Thus, the essence of problem is to solve the radiative transfer equation, which describes the temporal and spatial evolution of the radiation field J_ν :

$$1/c \frac{dI_\nu}{dt} + \frac{dI_\nu}{ds} = \eta_\nu - \alpha_\nu I_\nu \quad (1)$$

where ds is geometrical path length along the beam, η_ν and α_ν are the monochromatic (linear or volume) emission and extinction coefficients. Clearly, the transport of radiation depends on the medium in which it propagates. Thus, we also need a model that describes the thermodynamic properties in stellar atmospheres, which must include radiation transport.

There are several types of models, vastly different in complexity and computational burden: from the simplest 1D LTE hydrostatic models to the (presently) most sophisticated 3D RHD LTE models with scattering. In all cases, the radiative transfer is assumed to be *quasi-static*, i.e. the time derivative is neglected, which is not a bad approximation because the photon propagation time is much shorter than the fluid motion time. The computational timescales range from few seconds of CPU to several months. In the next section, I will summarise the main ingredients of all these model types without going into details of how the equations are solved (see e.g. Mihalas 1979).

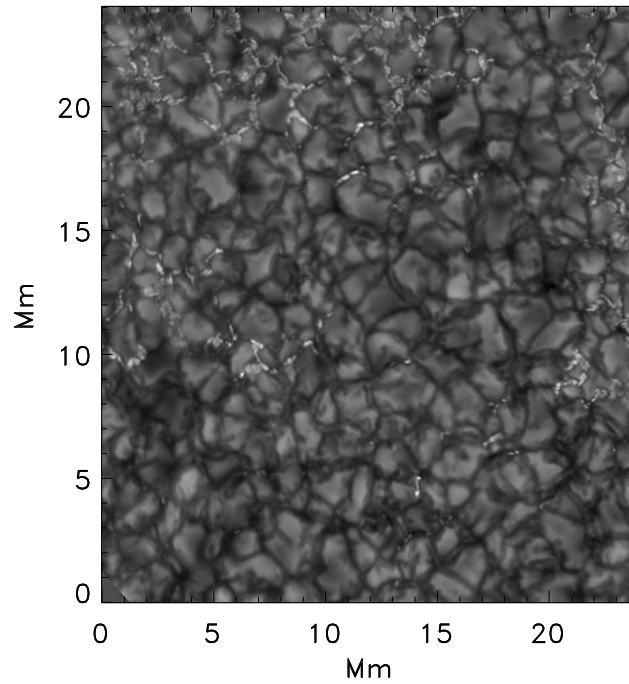


Fig. 1 Solar granulation in the G-continuum (Nordlund et al, 2009). Observations were made on the Swedish 1m Solar Telescope (Institute of Theoretical Astrophysics, Oslo). Reproduced by permission from the authors and the publisher.

3.1 Classical 1D static model atmospheres

The simplest models are computed using the 1D hydrostatic LTE approximations. We have to solve several equations:

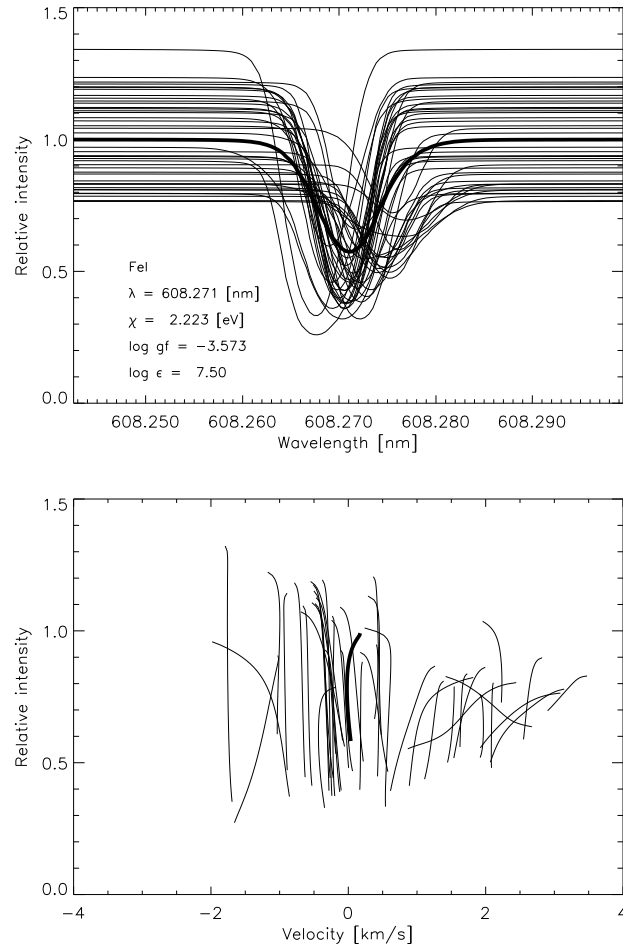


Fig. 2 Line profiles of the Fe I line at 6082 \AA in the 3D RHD simulations of the solar atmosphere (Asplund et al, 2000). Top panel: spatially-resolved profiles. Bottom panel: the line bisectors. The thick lines on both panels indicate the spatially-averaged profile and the C-shaped bisector. The line asymmetries are a consequence of blue- and red-shifts caused by the influence of the convective velocity fields on the line formation. Reproduced by permission from the authors and the publisher.

1. equation of radiative transfer in the static, time-independent, case. For a plane-parallel atmosphere with a geometrical depth z (it is straightforward to generalise this to a spherically-symmetric case):

$$\cos \theta \frac{dI_\nu}{dz} = \alpha_\nu I_\nu - \eta_\nu \quad (2)$$

The equation describes a change of specific intensity I_ν , as radiation passes through a slab of a thickness dz . For the plane-parallel approximation, the latter is represented by the projection at angle θ between the direction of the light beam and the z axis. The parameters α_ν and η_ν with dimensions cm^{-1} are the monochromatic linear extinction and emission coefficients; their ratio gives a source function $S_\nu = \frac{\eta_\nu}{\alpha_\nu}$. In LTE calculations, the source function is equal to the Planck function $S_\nu = B_\nu$ if only true absorption and emission processes are considered (strict LTE), or approximated by a two-level form, $S_\nu = (\kappa_\nu B_\nu + \sigma_\nu J_\nu) / (\kappa_\nu + \sigma_\nu)$, where κ is the true absorption and σ the scattering coefficients. In 'less strict' LTE, one may include, e.g. a coherent isotropic scattering in continuum, e.g. Thomson scattering on electrons e^- .

2. equation of flux constancy, or energy conservation:

$$F = \frac{L}{4\pi R^2} = \sigma T_{\text{eff}}^4, \quad (3)$$

where F is the bolometric flux, L the luminosity, R the stellar radius, and T_{eff} the effective temperature. In other words the divergence of the total energy flux transported to the surface is zero, $\nabla F = 0$ (see the next section on 3D RHD models), and the total flux is equated to the integral flux from the surface of a black body.

The total flux is usually taken to be the sum of convective and radiative components, $F = F_{\text{conv}} + F_{\text{rad}}$. The convective flux, F_{conv} , is needed because in deeper atmospheric layers, energy is mostly carried by convection. In the standard 'mixing-length' type approximations, $F_{\text{conv}} \sim \frac{\alpha_{MLT}}{H_p}$, where H_p is pressure scale height and α_{MLT} the mixing-length parameter. There are attempts to calibrate the mixing length parameter based on 3D models (see next Section).

3. radiative equilibrium equation¹:

$$\int_0^\infty \alpha_\nu J_\nu(\tau) d\nu = \int_0^\infty \alpha_\nu S_\nu(\tau) d\nu \quad (4)$$

where τ is the optical depth, J_ν the mean intensity averaged over all directions, and S_ν the source function. The left-hand side of the equation can be viewed as radiation 'sink' term, and right-hand side is the radiation 'source' term, which in LTE is usually equal to the Planck function (see the next section for how this is treated in 3D RHD models). In the calculations of energy balance with 1D hydrostatic models, it is presently possible to evaluate detailed opacity on more than 10^5 wavelength points (e.g. Gustafsson et al, 2008; Grupp, 2004). This samples the majority of the atomic and molecular lines, which contribute to the opacity under conditions typical of a late-type star.

4. equation of hydrostatic equilibrium:

¹ Assuming that energy is transported by radiation only.

$$\nabla P_{tot} = -\rho \frac{GM_r}{r^2}, \quad (5)$$

where ρ is the density, M_r mass at the radius r , $\nabla P_{tot} = \nabla P_{gas} + \nabla P_{rad}$, i.e the sum of gas and radiative pressures. The latter can be expressed as:

$$\nabla P_{rad} = -1/c \int_0^\infty (\kappa_\nu + \sigma_\nu) F_\nu d\nu \quad (6)$$

Gas pressure is balanced by the gravitational attraction, which does not change with depth in plane-parallel models. In spherically-symmetric models, $g = g(r)$, thus mass (M) and luminosity ($L = 4\pi r^2 F(r)$) are constant throughout the atmosphere. Note that there are some variations, e.g. some models include a turbulent pressure term, $\nabla P_{turb} \sim \rho v_t^2$, where v_t is the characteristic velocity, which may be used e. g. in very extended atmospheres (red giant branch or red supergiant stars) to approximate the levitation of the photosphere, the effect of 3D hydrodynamics. For detailed numerical schemes and practical implementation of the equations, the reader is referred to Kurucz (1993), Grupp (2004), Gustafsson et al (2008).

With the 1D hydrostatic approximation, it is also possible to compute fully-consistent NLTE models including the feedback on the atmospheric structure. Such models can be computed with the PHOENIX code (Baron and Hauschildt, 1998), which is very versatile in its applicability. In NLTE, PHOENIX includes more than 20 elements in the rate equations. NLTE model atmospheres, because of the UV overionization in Fe, lead to *warmer* outer atmospheric layers with respect to LTE for stars with $T_{\text{eff}} > \sim 5400$ K (Short and Hauschildt, 2005, 2009). However, surface cooling by ~ 150 K is predicted for the cooler stars, like the RGB star Arcturus (Fig. 3, top panel), which is caused by the UV over-ionisation in the bound-free edges of Mg, Si, and Al. This has a major impact on the UV fluxes of cool stars (Fig. 3, bottom panel).

3.2 3D RHD model atmospheres

Full time-dependent, 3D, RHD simulations of radiative and convective energy transport in stellar atmospheres exist since more than 2 decades. The seminal papers in this field are Nordlund (1982), Stein and Nordlund (1998), and Spruit et al (1990). 3D RHD models have substantially gained in complexity since then (e.g. Nordlund et al 2009, Chiavassa et al 2011, Collet et al 2011, Beeck et al 2012), in particular in the treatment of radiation transport. More details about the state-of-the-art models and their application to modelling stellar spectra will be given in the next section, here I only briefly review the equations of radiative hydrodynamics, needed to compute the models.

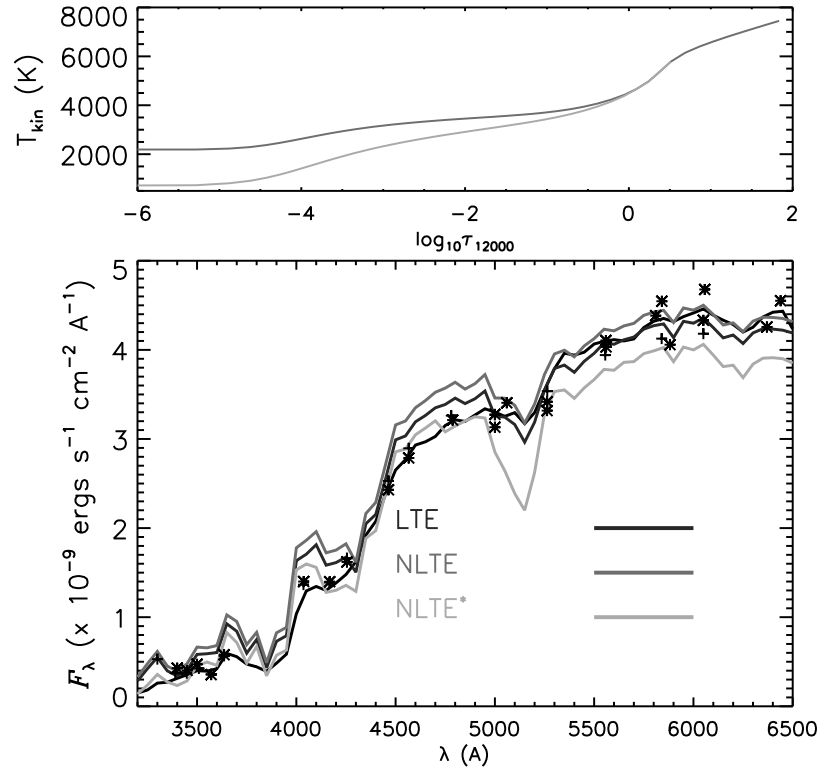


Fig. 3 NLTE model atmospheres (top) and synthetic spectra (bottom) for Arcturus, a very cool RGB star (dark - LTE, light - NLTE). NLTE* refers to the NLTE calculations with an ad-hoc kinetic temperature structure adjusted to fit the near-UV SED; note however that the fit in the optical has degraded. Reproduced by permission from the authors (Short and Hauschildt, 2009) and from the publisher.

The main difference with respect to hydrostatic models (see above) is that one solves time-dependent fluid-hydrodynamics equations for compressible fluid flow. In Eulerian form, the equations are:

1. the equation of continuity or mass conservation

$$\frac{\partial \rho}{\partial t} = -\nabla \cdot (\rho \mathbf{v}), \quad (7)$$

where $\mathbf{v} = \mathbf{v}(x, z, y, t)$ is the velocity vector. The equation essentially means that in the ascending flow, the rapid decrease of density can be balanced by the rapid expansion sideways.

2. equation of motion

$$\frac{\partial \rho \mathbf{v}}{\partial t} = -\nabla \cdot (\rho \mathbf{v} \mathbf{v}) - \nabla P - \rho \nabla \Phi - \nabla \cdot \tau_{visc}, \quad (8)$$

where P is the gas pressure, Φ the gravitational potential, τ_{visc} the viscous stress tensor. The first term on the right-hand side is the divergence of the vertical component of Reynold's stress tensor, i.e. the force density on the fluid due to the turbulent fluctuations. Under the assumption of slow and bulky fluid motions, one simply recovers the equation of hydrostatic equilibrium (eq. 5).

In the 'box-in-a-star' simulations, the gravitational potential is a constant, so $d\Phi/dz = -g$, surface gravity. Box-in-a-star simulations are usually applied to modelling solar-like stars (e.g. Stein and Nordlund, 1998).

In contrast, in the 'star-in-a-box' setup, the simulation box includes the whole star (e.g. Freytag et al, 2012). In the 'star-in-a-box' regime, one assumes a spherical potential in the form:

$$\Phi = -\frac{GM}{(r_0^4 + r^4/\sqrt{I} + (r/r_1)^8)^{1/4}} \quad (9)$$

where r_0 and r_1 are the so-called 'smoothing parameters'. They provide limiting values of gravitational potential for $r \rightarrow 0$ and $r \rightarrow \infty$. For large stars-in a box models, $r_0 \sim 0.2 R_{star}$. This setup is applied to model very extended, variable and stochastically pulsating stars, such as cool giants and red supergiants. Note that the size of granules is very different for solar-like and giant stars, it scales with the pressure scale height (Freytag et al, 2002).

3. energy conservation

$$\frac{\partial E}{\partial t} = -\nabla \cdot (\mathbf{v}(E_i + P)) - \frac{1}{2} \nabla \cdot \rho v^2 \mathbf{v} + Q_{rad} + Q_{visc} \quad (10)$$

where E is the total energy density, i.e. the sum of internal E_i and kinetic E_{kin} energies, Q_{visc} is the viscous dissipation term and Q_{rad} is the radiative term, which is expressed as:

$$Q_{rad} = -\nabla \cdot F_{rad} = 4\pi \int_0^\infty \alpha_\nu (I_\nu - S_\nu) d\Omega d\nu \quad (11)$$

here the intensity I comes from the solution of radiation transport equation, which is done separately on a system of rays for different outgoing directions. Radiative transfer calculations are very expensive in 3D, because it is necessary to compute several radiative ray directions for every convective time step in the RHD computation. Therefore the radiation field is computed using opacity bins, which are constructed by sorting all (line plus continuum) opacities into groups according

to their amplitude (Nordlund, 1982):

$$Q_{\text{rad}} \equiv \sum_{n=1, n_{\text{bins}}} (J_{\text{bin}} - B_{\text{bin}}) w_{\text{bin}}, \quad (12)$$

where J and B are the mean intensity and the Planck function, and each quantity in this equation refers to a 'bin' rather than to a wavelength. w_{bin} is the weight of each bin, computed as a sum of the weights of individual wavelength points in a bin. Note that in this definition, one assumes that the Planck function does not vary much across a bin. Modern codes (such as Stagger) use up to 12 opacity bins, which sort the opacities according to magnitude and wavelength.

There are several codes available for 3D RHD modelling: the Copenhagen Stagger code (Nordlund and Galsgaard, 1992), MuRAM (Vögler et al, 2005), BIFROST (Gudiksen et al, 2011), CO5BOLD (Freytag et al, 2012; Chiavassa et al, 2011), ANTARES (Muthsam et al, 2010). All these codes are capable of simulating stellar convection in the box-in-a-star regime. The CO5BOLD code also supports the star-in-a-box simulations of stellar convection.

In the box-in-a-star regime, the physical domains of the simulations cover a representative portion of the stellar surface. Vertically, they include the whole photosphere as well as the upper part of the convective layers, typically encompassing 12 to 15 pressure scale heights. Horizontally, they extend over an area sufficiently large to host at least about ten granules at the surface. Fig. 4 shows a snapshot from a 3D RHD simulation of the solar surface convection. The granule characterised by warm up flowing material is surrounded by cooler inter granular lanes, in which material sinks under the influence of gravity. Such models predict a different temperature and pressure structure of a stellar atmosphere, especially for stellar parameters different from the Sun. For example, at low metallicity, 1D hydrostatic models severely overestimate the average temperatures of the upper atmospheric layers, with profound implications for the spectral line formation (e.g. Collet et al, 2007).

One may also use 3D RHD models to devise smart calibration relationships, which can be applied in 1D hydrostatic computations to better approximate the complex physical processes. One of the most interesting applications is the calibration of the *mixing-length parameter*, α_{MLT} . Fig. 5 shows the behaviour of α with the effective temperature T_{eff} and surface gravity $\log g$. The T_{eff} -scale is logarithmic. Evolutionary tracks (Paxton et al, 2011) are also indicated. The α -values are indicated with colours. The solar simulation is indicated with a \odot and the locations of the other simulations are shown with asterisks. In all 1D hydrostatic models (such as MARCS, Kurucz, MAFAGS), the mixing-length is constant, and, depending on the formulation (e.g. Böhm-Vitense 1958, or Canuto and Mazzitelli 1991), it takes values from 0.5 to 1.5. From Fig. 5, it is obvious that none of these factors are physically sensible across the full HRD. At best, a constant α could be used for the stars very similar to the Sun, but not for any other star.

Grids of 3D models have been presented in Tanner et al (2013, 14 models), Trampedach et al (2013, 37 models), Ludwig et al (2009, 77 models), Magic et al (2013, 202 models). Also, spatial and temporal averages of the full RHD models

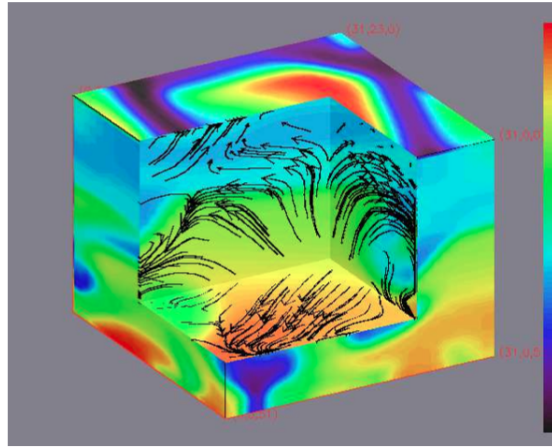


Fig. 4 A granule in the simulation of the solar convection. The colour bar indicates temperature. By permission from the authors (Nordlund et al, 2009) and from the publisher.

have been constructed; such models facilitate calculation of large grids of synthetic spectra at a reasonable computation cost thus allowing to apply them in problems of stellar abundance analysis (e.g. Caffau et al, 2011; Bergemann et al, 2012; Tremblay et al, 2013).

StaggerGrid project (Collet et al, 2011) is a collaborative project for the construction of a comprehensive grid of time-dependent 3D RHD model atmospheres of solar- and late-type stars. The project involves several research groups and different RHD codes.

4 Line formation and spectrum synthesis

Once we have a model providing basic thermodynamic quantities of an atmosphere as a function of depth, it is straightforward to calculate the emergent stellar spectra. The model spectra are then directly compared with observations and stellar parameters can be determined from the best-fit templates (Fig. 6).

4.1 LTE spectrum synthesis

In LTE, the calculation of model spectra can be easily done in 1D or 3D geometry, by computing the formal solution of the radiative transfer equation along a series of rays at different μ angles using the long- or short-characteristics methods (see e.g.

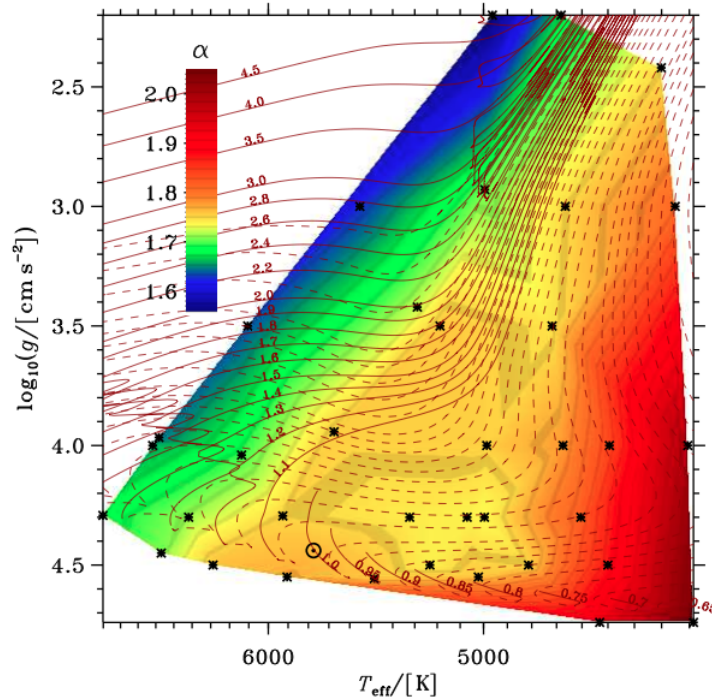


Fig. 5 The behavior of the calibrated MLT α with T_{eff} and g_{surf} (Fig. courtesy of R. Trampedach, see also Trampedach et al 2013). The T_{eff} -scale is logarithmic. We have also plotted evolutionary tracks produced with the MESA-code (Paxton et al, 2011), covering the mass-range $0.65 - 4.5 M_{\odot}$, as indicated. The dashed lines correspond to the pre-main-sequence evolution. The α -values were interpolated linearly on Thiessen triangles between the simulations, and indicate the values with colors as shown on the color bar. The solar simulation is indicated with a \odot and the locations of the other simulations are shown with asterisks.

Hauschildt and Baron 2006). Long characteristics is preferred for detailed line profiles, while short characteristics is used for solving approximate radiation transport in 3D RH simulations. If scattering is included, iterative solutions are needed, such as variable Eddington factor (Auer and Mihalas, 1970).

In 1D LTE, very efficient and well-tested codes to compute full synthetic spectra are SIU (Reetz 1999, Schoenrich and Bergemann 2013) and Turbospectrum (Alvarez and Plez, 1998; Plez, 2012), SYNTHE (Kurucz, 2005). These codes were used to compute full libraries of synthetic spectra (e.g. Murphy and Meiksin, 2004; de Laverny et al, 2012) for stellar spectroscopy or population synthesis.

Codes that are able to compute 3D line formation in LTE include SCATE (Hayek et al, 2011), Optim3D (Chiavassa et al, 2009), ASSET (Koesterke et al, 2008), Linfor3D (Cayrel et al, 2007). These codes can potentially be used to compute full

3D grids of synthetic spectra. For example, a grid of 3D synthetic spectra has been recently presented by Allende Prieto et al (2013).

Fig. 7 shows the CN lines computed with a 3D RHD model of a metal-poor giant, in comparison with the 1D hydrostatic model (Collet in prep.). In addition to a different temperature structure, temperature and pressure fluctuations in the 3D models contribute strictly positively to the molecular number density (Uitenbroek and Criscuoli, 2011), that is why the abundance derived from molecular lines is lower. In Fig. 7, the CN lines in 3D provide a -0.4 dex lower abundances compared to the 1D result.

4.2 NLTE

In NLTE, the problem of radiative transfer and thus modelling a spectrum is much more complex. Radiative transfer shall be solved simultaneously with the rate equations, the latter provide coupling between non-local radiation field and local properties of the gas.

$$\frac{\partial n_i}{\partial t} + \nabla \cdot (n_i \mathbf{v}) = \sum_{j \neq i} n_j P_{ji} - n_i \sum_{j \neq i} P_{ij} \quad (13)$$

where n is the number density of species of a certain type (e.g. atoms on the excitation state i), P the total transition rates (radiative plus collisional) between the states.

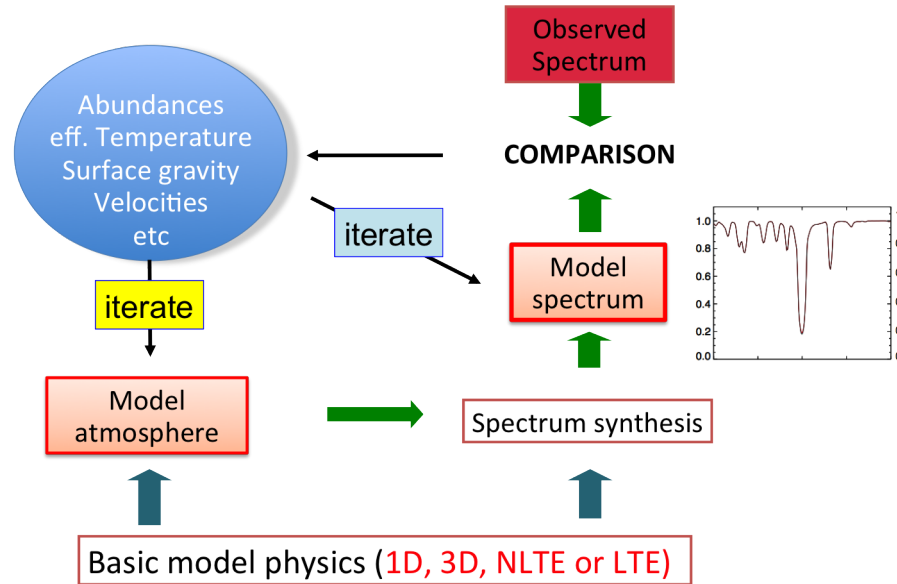


Fig. 6 The basic flow chart of spectroscopic analysis .

In the time-independent case, the left-hand term can be neglected and we recover the statistical equilibrium (SE) equations. Even in the 1D hydrostatic case, the solution of the RT and SE requires very efficient numerical schemes. In 1D, the most widely-used codes are DETAIL (Butler and Giddings 1985 and the updated version by Bergemann et al 2012b) and MULTI (Carlsson, 1992). The codes are stable and efficient. Presently, they are most useful for the diagnostics and detailed analysis of NLTE effects, especially for complex multi-electron atomic systems, like Fe I, and applications to stellar parameter and abundance analysis of large datasets.

In 3D, MULTI3D (Botnen and Carlsson, 1999; Leenaarts and Carlsson, 2009) and MUGA (Auer et al, 1994) are frequently used for the analysis of stellar observations. The codes have been already applied to solve line transfer problems in the Sun and late-type stars. For example, Fig. 8 shows how the Li I line strength varies across the surface of star in a 3D radiation-hydrodynamic simulation (Lind et al, 2013). Other interesting applications of the fully 3D NLTE framework include Asplund et al (2003, Li I), Cayrel et al (2007, Li I), Asplund et al (2004, O I), Trujillo Bueno and Shchukina (2007, Sr I), Leenaarts et al (2009, Ca II), (Lind et al, 2013, Ca I, Na I). It is now also possible to perform NLTE line formation with the temporal and spatial averages of 3D models, such as done by Bergemann et al (2012) for Fe I and Bergemann et al (2013) for Ti I and Si I lines.

In general, NLTE effects on spectral line formation are well-understood for most of the chemical elements. The majority of species, for which spectral lines are observed in the spectra of FGKM stars, are affected by NLTE over-ionization. That means, the NLTE lines are weaker, especially if they are on the linear part of the curve-of-growth. In this case, the NLTE effects on the ionisation balance are typically large for giants and metal-poor stars (e.g. Bergemann et al, 2012). Resonance line scattering is relevant for strong lines of singly-ionised elements (Ba II, Sr II: Bergemann et al, 2012a; Shchukina et al, 2009). Atomic lines of neutral species in the IR may show emission line cores (Carlsson and Rutten, 1992; Carlsson et al, 1992). A detailed discussion of the NLTE effects in the spectral lines of different elements can be found in Mashonkina (2013).

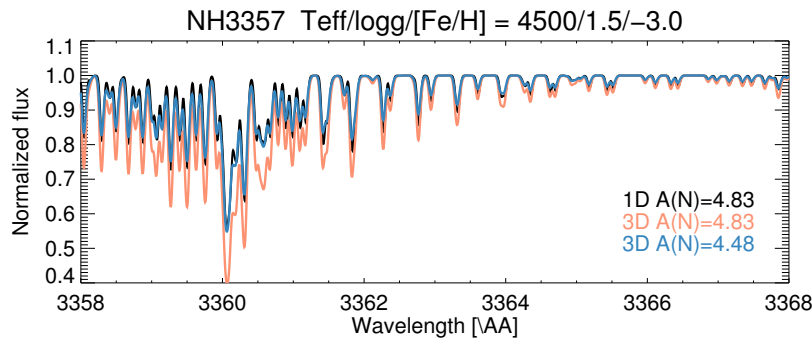


Fig. 7 CN lines computed with a 3D RHD model of a metal-poor star (Collet et al. in prep).

While the detailed solution of NLTE radiative transfer in 1D is straightforward, this is not always simple, especially when it concerns stellar abundance analysis. The most difficult task is usually to assemble a comprehensive model atom using the best atomic data available for a given element. This involves mining large atomic databases, like TOPbase and Kurucz web-servers, NIST, VALD; it is even more difficult to homogenise the atomic information, e.g. electronic configurations and level energies, particularly when the combination of quantum-mechanical and experimental data is needed to ensure the completeness of the model atom. For those workers in the field of observational stellar astrophysics, who are not directly involved in the development of NLTE radiative transfer models, this is a difficult undertaking.

A simpler approach has been developed, which allows to bypass difficult statistical equilibrium calculations. The idea is to use *NLTE abundance corrections*, which can be pre-computed for a large grid of model atmospheres and element abundances. The NLTE abundance correction is then applied to a best-fit LTE abundance. Numerous tests showed that the accuracy of NLTE element abundances obtained by this method is very good.

NLTE abundance correction for a given chemical element, Δ_{El} , is defined as:

$$\Delta_{\text{El}} = \log A(\text{El})_{\text{NLTE}} - \log A(\text{El})_{\text{LTE}} \quad (14)$$

i.e., it is the logarithmic correction, which has to be applied to an LTE abundance determination A of a specific line to obtain the correct value corresponding to the use of NLTE line formation.

INSPECT² is the first project, which allows one to compute NLTE corrections online; one may also request LTE or NLTE abundance for a measured equivalent width of a spectral line, provided stellar parameters are known. The following species are available: Li I, Na I, Ti I, Fe I/II, Sr II. Smaller databases of NLTE corrections are also provided in the literature (e.g., Bergemann and Gehren 2008: Mn I, Merle et al 2011: Mg I, Ca I).

5 Conclusions

We are now entering the new era of observational stellar astrophysics, moving away from 1D hydrostatic models with LTE - which is known as 'classical' approach - to 3D radiative hydrodynamics with non-LTE. The transition is slow, mostly because of the associated computational challenges. However, the need for more realistic models, which provide more accurate and un-biased results, i.e. fundamental stellar parameters and element abundances, is now as urgent as never before. Large-scale

² www.inspect-stars.net

stellar surveys (like Gaia-ESO and APOGEE) provide observed spectra of unprecedented quality and pave the way to massive applications of the new models. From the recent developments in theory, it seems that most promising approach is to compute NLTE line formation with the averages of full 3D RHD models.

Acknowledgements Figure 1 reproduced by permission of the authors; the image was observed with the Swedish 1-m Solar Telescope. The SST is operated on the island of La Palma by the Institute for Solar Physics in the Spanish Observatorio del Roque de los Muchachos of the Instituto de Astrofísica de Canarias. The Institute for Solar Physics is a national research infrastructure under the Swedish Research Council. It is managed as an independent institute associated with Stockholm University through its Department of Astronomy. Figure 2: Asplund et al. *A&A*, 359, 729, 2000, reproduced with permission (c) ESO. Figures 3, 4 reproduced by permission of the AAS. Figure 8: Lind et al. *A&A*, 554, A96, 2013, reproduced with permission (c) ESO. We thank R. Collet and R. Trampedach for the figures from the papers in preparation, and K. Lind for the useful comments to the manuscript. This work was partly supported by the European Union FP7 programme through ERC grant number 320360.

References

- Allende Prieto C, Koesterke L, Ludwig HG, Freytag B, Caffau E (2013) Convective line shifts for the Gaia RVS from the CIFIST 3D model atmosphere grid. *Astronomy & Astrophysics* 550:A103, DOI 10.1051/0004-6361/201220064, 1301.3703
- Alvarez R, Plez B (1998) Near-infrared narrow-band photometry of M-giant and Mira stars: models meet observations. *Astronomy & Astrophysics* 330:1109–1119
- Asplund M (2005) New Light on Stellar Abundance Analyses: Departures from LTE and Homogeneity. *Annual Review of Astronomy and Astrophysics* 43(1):481–530
- Asplund M, Nordlund A, Trampedach R, Allende Prieto C, Stein RF (2000) Line formation in solar granulation. I. Fe line shapes, shifts and asymmetries. *Astronomy & Astrophysics* 359:729–742
- Asplund M, Carlsson M, Botnen AV (2003) Multi-level 3D non-LTE computations of lithium lines in the metal-poor halo stars HD 140283 and HD 84937. *Astronomy & Astrophysics* 399:L31–L34, DOI 10.1051/0004-6361:20030080, astro-ph/0302406
- Asplund M, Grevesse N, Sauval AJ, Allende Prieto C, Kiselman D (2004) Line formation in solar granulation. IV. [O I], O I and OH lines and the photospheric O abundance. *Astronomy & Astrophysics* 417:751–768, DOI 10.1051/0004-6361:20034328, astro-ph/0312290
- Auer L, Bendicho PF, Trujillo Bueno J (1994) Multidimensional radiative transfer with multilevel atoms. 1: ALI method with preconditioning of the rate equations. *Astronomy & Astrophysics* 292:599–615

- Auer LH, Mihalas D (1970) On the use of variable Eddington factors in non-LTE stellar atmospheres computations. *Monthly Notices of the Royal Astronomical Society* 149:65
- Baron E, Hauschildt PH (1998) Parallel Implementation of the PHOENIX Generalized Stellar Atmosphere Program. II. Wavelength Parallelization. *The Astrophysical Journal* 495(1):370–376
- Beeck B, Collet R, Steffen M, Asplund M, Cameron RH, Freytag B, Hayek W, Ludwig HG, Schüssler M (2012) Simulations of the solar near-surface layers with the CO5BOLD, MURaM, and Stagger codes. *Astronomy & Astrophysics* 539:A121
- Bergemann M, Gehren T (2008) NLTE abundances of Mn in a sample of metal-poor stars. *Astronomy & Astrophysics* 492:823–831, DOI 10.1051/0004-6361/200810098, 0811.0681
- Bergemann M, Hansen CJ, Bautista M, Ruchti G (2012a) NLTE analysis of Sr lines in spectra of late-type stars with new R-matrix atomic data. *Astronomy & Astrophysics* 546:A90, DOI 10.1051/0004-6361/201219406, 1207.2451
- Bergemann M, Kudritzki RP, Plez B, Davies B, Lind K, Gazak Z (2012b) Red Supergiant Stars as Cosmic Abundance Probes: NLTE Effects in J-band Iron and Titanium Lines. *The Astrophysical Journal* 751:156, DOI 10.1088/0004-637X/751/2/156, 1204.0511
- Bergemann M, Lind K, Collet R, Magic Z, Asplund M (2012) Non-LTE line formation of Fe in late-type stars – I. Standard stars with 1D and 3D model atmospheres. *Monthly Notices of the Royal Astronomical Society* 427(1):27–49
- Bergemann M, Kudritzki RP, Davies B, Plez B, Gazak Z, Chiavassa A (2013) 3D NLTE line formation in the atmospheres of red supergiants. In: Kervella P, Le Bertre T, Perrin G (eds) *EAS Publications Series*, *EAS Publications Series*, vol 60, pp 103–109, DOI 10.1051/eas/1360011, 1303.4768
- Böhm-Vitense E (1958) Über die Wasserstoffkonvektionszone in Sternen verschiedener Effektivtemperaturen und Leuchtkräfte. Mit 5 Textabbildungen. *Zeitschrift für Astrophysik* 46:108
- Botnen A, Carlsson M (1999) Multi3D, 3D Non-LTE Radiative Transfer. In: Miyama SM, Tomisaka K, Hanawa T (eds) *Numerical Astrophysics*, *Astrophysics and Space Science Library*, vol 240, p 379
- Buscher DF, Baldwin JE, Warner PJ, Haniff CA (1990) Detection of a bright feature on the surface of Betelgeuse. *Monthly Notices of the Royal Astronomical Society* 245:7P–11P
- Butler K, Giddings J (1985) *Newsletter on Analysis of Astronomical Spectra*, University of London 9
- Caffau E, Ludwig HG, Steffen M, Freytag B, Bonifacio P (2011) Solar Chemical Abundances Determined with a CO5BOLD 3D Model Atmosphere. *Solar Physics* 268:255–269, DOI 10.1007/s11207-010-9541-4, 1003.1190
- Canuto VM, Mazzitelli I (1991) Stellar turbulent convection - A new model and applications. *The Astrophysical Journal* 370:295–311
- Carlsson M (1992) The MULTI Non-LTE Program (Invited Review). In: Giampapa MS, Bookbinder JA (eds) *Cool Stars, Stellar Systems, and the Sun*, *Astronomical Society of the Pacific Conference Series*, vol 26, p 499

- Carlsson M, Rutten RJ (1992) Solar hydrogen lines in the infrared. *Astronomy and Astrophysics* (ISSN 0004-6361) 259:L53–L56
- Carlsson M, Rutten RJ, Shchukina NG (1992) The formation of the MG I emission features near 12 microns. *Astronomy and Astrophysics* (ISSN 0004-6361) 253:567–585
- Cayrel R, Steffen M, Chand H, Bonifacio P, Spite M, Spite F, Petitjean P, Ludwig HG, Caffau E (2007) Line shift, line asymmetry, and the 6Li/7Li isotopic ratio determination. *Astronomy & Astrophysics* 473:L37–L40, DOI 10.1051/0004-6361:20078342, 0708.3819
- Chiavassa A, Plez B, Josselin E, Freytag B (2009) Radiative hydrodynamics simulations of red supergiant stars. *Astronomy & Astrophysics* 506(3):1351–1365
- Chiavassa A, Freytag B, Masseron T, Plez B (2011) Radiative hydrodynamics simulations of red supergiant stars. *Astronomy & Astrophysics* 535:A22
- Collet R, Asplund M, Trampedach R (2007) Three-dimensional hydrodynamical simulations of surface convection in red giant stars. Impact on spectral line formation and abundance analysis. *Astronomy & Astrophysics* 469:687–706, DOI 10.1051/0004-6361:20066321, arXiv:astro-ph/0703652
- Collet R, Magic Z, Asplund M (2011) The StaggerGrid project: a grid of 3-D model atmospheres for high-precision spectroscopy. *Journal of Physics: Conference Series* 328(1):012,003
- de Laverny P, Recio-Blanco A, Worley CC, Plez B (2012) The AMBRE project: A new synthetic grid of high-resolution FGKM stellar spectra. *Astronomy & Astrophysics* 544:A126, DOI 10.1051/0004-6361/201219330, 1205.2270
- Freytag B, Steffen M, Dorch B (2002) Spots on the surface of Betelgeuse – Results from new 3D stellar convection models. *Astronomische Nachrichten* 323:213–219
- Freytag B, Steffen M, Ludwig HG, Wedemeyer-Böhm S, Schaffenberger W, Steiner O (2012) Simulations of stellar convection with CO5BOLD. *Journal of Computational Physics* 231:919–959, DOI 10.1016/j.jcp.2011.09.026, 1110.6844
- Gray DF, Carney BW, Yong D (2008) Asymmetries in the Spectral Lines of Evolved Halo Stars. *The Astronomical Journal* 135:2033–2037, DOI 10.1088/0004-6256/135/6/2033
- Grupp F (2004) MAFAGS-OS: New opacity sampling model atmospheres for A, F and G stars. *Astronomy & Astrophysics* 426(1):309–322
- Gudiksen BV, Carlsson M, Hansteen VH, Hayek W, Leenaarts J, Martínez-Sykora J (2011) The stellar atmosphere simulation code Bifrost. Code description and validation. *Astronomy & Astrophysics* 531:A154, DOI 10.1051/0004-6361/201116520
- Gustafsson B, Edvardsson B, Eriksson K, Jørgensen UG, Nordlund A, Plez B (2008) A grid of MARCS model atmospheres for late-type stars. *Astronomy & Astrophysics* 486(3):951–970
- Hansteen VH, Carlsson M, Gudiksen B (2007) 3D Numerical Models of the Chromosphere, Transition Region, and Corona. *The Physics of Chromospheric Plasmas* 368:107

- Haubois X, Perrin G, Lacour S, Verhoelst T, Meimon S, Mugnier L, Thiébaud E, Berger JP, Ridgway ST, Monnier JD, Millan-Gabet R, Traub W (2009) Imaging the spotty surface of Betelgeuse in the H band. *Astronomy & Astrophysics* 508:923–932, DOI 10.1051/0004-6361/200912927, 0910.4167
- Hauschildt PH, Baron E (2006) A 3D radiative transfer framework. *Astronomy & Astrophysics* 451(1):273–284
- Hayek W, Asplund M, Collet R, Nordlund A (2011) 3D LTE spectral line formation with scattering in red giant stars. *Astronomy & Astrophysics* 529:A158
- Höfner S, Gautschi-Loidl R, Aringer B, Andersen A, Jørgensen UG (2003) Dynamical Atmospheres and Winds of AGB Stars. *Astronomische Nachrichten Supplement* 324:19
- Kervella P, Verhoelst T, Ridgway ST, Perrin G, Lacour S, Cami J, Haubois X (2009) The close circumstellar environment of Betelgeuse. *Astronomy & Astrophysics* 504(1):115–125
- Koesterke L, Allende Prieto C, Lambert DL (2008) Center-to-Limb Variation of Solar Three-dimensional Hydrodynamical Simulations. *The Astrophysical Journal* 680(1):764–773
- Kurucz RL (1993) A New Opacity-Sampling Model Atmosphere Program for Arbitrary Abundances. *The Physics of Chromospheric Plasmas* 44:87
- Kurucz RL (2005) ATLAS12, SYNTHE, ATLAS9, WIDTH9, et cetera. *Memorie della Societa Astronomica Italiana* 8:14
- Leenaarts J, Carlsson M (2009) MULTI3D: A Domain-Decomposed 3D Radiative Transfer Code. In: Lites B, Cheung M, Magara T, Mariska J, Reeves K (eds) *The Second Hinode Science Meeting: Beyond Discovery-Toward Understanding*, *Astronomical Society of the Pacific Conference Series*, vol 415, p 87
- Leenaarts J, Carlsson M, Hansteen V, Rouppe van der Voort L (2009) Three-Dimensional Non-LTE Radiative Transfer Computation of the CA 8542 Infrared Line From a Radiation-MHD Simulation. *The Astrophysical Journal* 694:L128–L131, DOI 10.1088/0004-637X/694/2/L128, 0903.0791
- Lind K, Melendez J, Asplund M, Collet R, Magic Z (2013) The lithium isotopic ratio in very metal-poor stars. *Astronomy & Astrophysics* 554:A96
- Lucy LB (1999) Computing radiative equilibria with Monte Carlo techniques. *Astronomy & Astrophysics* 344:282–288
- Ludwig HG, Caffau E, Steffen M, Freytag B, Bonifacio P, Kučinskas A (2009) The CIFIST 3D model atmosphere grid. *Mem. Societa Astronomica Italiana* 80:711, 0908.4496
- Magic Z, Collet R, Asplund M, Trampedach R, Hayek W, Chiavassa A, Stein RF, Nordlund A (2013) The Stagger-grid: A grid of 3D stellar atmosphere models. *Astronomy & Astrophysics* 557:A26
- Mashonkina L (2013) Review: progress in NLTE calculations and their application to large data-sets. *ArXiv e-prints* 1306.6426
- Merle T, Thévenin F, Pichon B, Bigot L (2011) A grid of non-local thermodynamic equilibrium corrections for magnesium and calcium in late-type giant and supergiant stars: application to Gaia. *Monthly Notices of the Royal Astronomical Society* 418:863–887, DOI 10.1111/j.1365-2966.2011.19540.x, 1107.6015

- Mihalas D (1979) Book-Review - Stellar Atmospheres. *Soviet Astronomy* 23:386
- Mihalas D, Athay RG (1973) The Effects of Departures from LTE in Stellar Spectra. *Annual Review of Astronomy and Astrophysics* 11(1):187–218
- Murphy T, Meiksin A (2004) A library of high-resolution Kurucz spectra in the range $\lambda\lambda 3000$ – $10\ 000$. *Monthly Notices of the Royal Astronomical Society* 351:1430–1438, DOI 10.1111/j.1365-2966.2004.07895.x, astro-ph/0404010
- Muthsam HJ, Kupka F, Löw-Baselli B, Obertscheider C, Langer M, Lenz P (2010) ANTARES – A Numerical Tool for Astrophysical RESearch with applications to solar granulation. *New Astronomy* 15(5):460–475
- Nordlund A (1982) Numerical simulations of the solar granulation. I - Basic equations and methods. *Astronomy & Astrophysics* 107:1–10
- Nordlund Å, Galsgaard K (1992) Large scale simulations. In: *Electromechanical Coupling of the Solar Atmosphere*, AIP, pp 13–23
- Nordlund Å, Stein RF, Asplund M (2009) Solar Surface Convection. *Living Reviews in Solar Physics* 6:2
- Ohnaka K, Hofmann KH, Benisty M, Chelli A, Driebe T, Millour F, Petrov R, Schertl D, Stee P, Vakili F, Weigelt G (2009) Spatially resolving the inhomogeneous structure of the dynamical atmosphere of Betelgeuse with VLTI/AMBER. *Astronomy & Astrophysics* 503:183–195, DOI 10.1051/0004-6361/200912247, 0906.4792
- Ohnaka K, Weigelt G, Millour F, Hofmann KH, Driebe T, Schertl D, Chelli A, Massi F, Petrov R, Stee P (2011) Imaging the dynamical atmosphere of the red supergiant Betelgeuse in the CO first overtone lines with VLTI/AMBER. *Astronomy & Astrophysics* 529:A163, DOI 10.1051/0004-6361/201016279, 1104.0958
- Paxton B, Bildsten L, Dotter A, Herwig F, Lesaffre P, Timmes F (2011) Modules for experiments in stellar astrophysics (MESA). *ApJS* 192(1):3:1–35
- Plez B (2012) Turbospectrum: Code for spectral synthesis. *Astrophysics Source Code Library*, 1205.004
- Reetz J (1999) Oxygen Abundances in Cool Stars and the Chemical Evolution of the Galaxy
- Schoenrich R, Bergemann M (2013) Fundamental stellar parameters and metallicities from Bayesian spectroscopy. Application to low- and high-resolution spectra. eprint arXiv:13115558
- Shchukina NG, Olshevsky VL, Khomenko EV (2009) The solar Ba II 4554 Å line as a Doppler diagnostic: NLTE analysis in 3D hydrodynamical model. *Astronomy & Astrophysics* 506:1393–1404, DOI 10.1051/0004-6361/200912048, 0905.0985
- Short CI, Hauschildt PH (2005) A NonLTE LineBlanketed Model of a SolarType Star. *The Astrophysical Journal* 618(2):926–938
- Short CI, Hauschildt PH (2009) NON-LTE MODELING OF THE NEAR-ULTRAVIOLET BAND OF LATE-TYPE STARS. *The Astrophysical Journal* 691(2):1634–1647
- Spruit HC, Nordlund A, Title AM (1990) Solar Convection. *Annual Review of Astronomy and Astrophysics* 28(1):263–303

- Stein RF, Nordlund A (1998) Simulations of Solar Granulation. I. General Properties. *Astrophysical Journal* v499 499:914
- Tanner JD, Basu S, Demarque P (2013) VARIATION OF STELLAR ENVELOPE CONVECTION AND OVERSHOOT WITH METALLICITY. *The Astrophysical Journal* 767(1):78
- Teyssier D, Quintana-Lacaci G, Marston AP, Bujarrabal V, Alcolea J, Cernicharo J, Decin L, Dominik C, Justtanont K, de Koter A, Melnick G, Menten KM, Neufeld DA, Olofsson H, Planesas P, Schmidt M, Soria-Ruiz R, Schöier FL, Szczerba R, Waters LBFM (2012) Herschel/HIFI observations of red supergiants and yellow hypergiants. *Astronomy & Astrophysics* 545:A99
- Trampedach R, Asplund M, Collet R, Nordlund Å, Stein RF (2013) A Grid of Three-dimensional Stellar Atmosphere Models of Solar Metallicity. I. General Properties, Granulation, and Atmospheric Expansion. *The Astrophysical Journal* 769:18, DOI 10.1088/0004-637X/769/1/18, 1303.1780
- Tremblay PE, Ludwig HG, Freytag B, Steffen M, Caffau E (2013) Granulation properties of giants, dwarfs, and white dwarfs from the CIFIST 3D model atmosphere grid. *Astronomy & Astrophysics* 557:A7, DOI 10.1051/0004-6361/201321878, 1307.2810
- Trujillo Bueno J, Shchukina N (2007) The Scattering Polarization of the Sr I λ 4607 Line at the Diffraction Limit Resolution of a 1 m Telescope. *The Astrophysical Journal* 664:L135–L138, DOI 10.1086/520838, 0706.2386
- Tuthill PG, Haniff CA, Baldwin JE (1997) Hotspots on late-type supergiants. *Monthly Notices of the Royal Astronomical Society* 285:529–539
- Uitenbroek H, Criscuoli S (2011) WHY ONE-DIMENSIONAL MODELS FAIL IN THE DIAGNOSIS OF AVERAGE SPECTRA FROM INHOMOGENEOUS STELLAR ATMOSPHERES. *The Astrophysical Journal* 736(1):69
- Vögler A, Shelyag S, Schüssler M, Cattaneo F, Emonet T, Linde T (2005) Simulations of magneto-convection in the solar photosphere. Equations, methods, and results of the MURaM code. *Astronomy & Astrophysics* 429:335–351, DOI 10.1051/0004-6361:20041507
- Wilson RW, Baldwin JE, Buscher DF, Warner PJ (1992) High-resolution imaging of Betelgeuse and Mira. *Monthly Notices of the Royal Astronomical Society* 257:369–376
- Wilson RW, Dhillon VS, Haniff CA (1997) The changing face of Betelgeuse. *Monthly Notices of the Royal Astronomical Society* 291:819
- Young JS, Baldwin JE, Boysen RC, Haniff CA, Lawson PR, Mackay CD, Pearson D, Rogers J, St-Jacques D, Warner PJ, Wilson DMA, Wilson RW (2000) New views of Betelgeuse: multi-wavelength surface imaging and implications for models of hotspot generation. *Monthly Notices of the Royal Astronomical Society* 315:635–645, DOI 10.1046/j.1365-8711.2000.03438.x

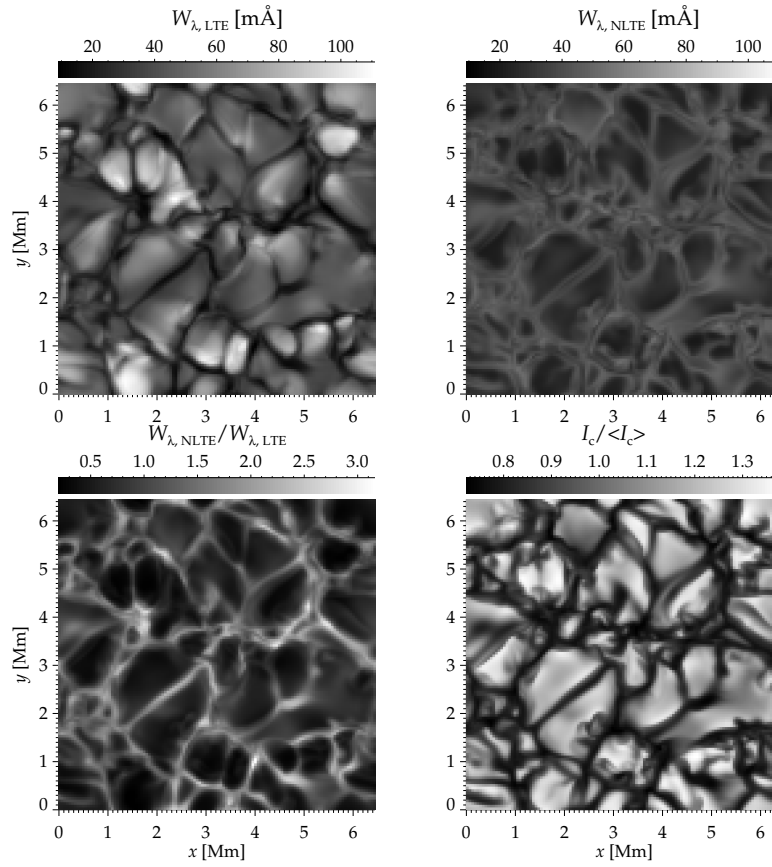


Fig. 8 Variation of the equivalent width for a Li I line at 6707 Å across a surface of a metal-poor star; the NLTE radiative transfer was computed using the 3D RHD simulation (Lind et al, 2013). Reproduced from permission by the author and the publisher.